Supporting Information

Synthesis of a Series of Rare-Earth-based Multi Anion Chalcogenide Iodides: $RE_3Si_2Se_xS_{8-x}I$ (RE = La, Ce, Pr, and Nd) Flux-Assisted Boron Chalcogen Mixture Method Crystal Growth and Characterization of Magnetic, Optical, and Photoluminescent Properties

Gopabandhu Panigrahi, Habiba B. Kashem, Gregory Morrison, and Hans-Conrad zur Loye*

Department of Chemistry and Biochemistry, University of South Carolina, Columbia, SC, 29208, United States

*E-mail: zurloye@mailbox.sc.edu

Table S1. Semi-quantitative elemental compositions determined by EDS.

	$La_3Si_2Se_{1.21}S_{6.79}I$				
Element	La	Si	Se	S	I
Weight%	43.3	7.2	13.2	23.1	13.2
Atomic%	20.0	16.4	10.7	46.2	6.7
	$Ce_3Si_2Se_{1.39}S_{6.61}I$				
Element	Ce	Si	Se	S	I
Weight%	46.3	6.8	10.2	23.5	13.2
Atomic%	22.1	14.4	10.6	46.2	6.7
	$Pr_3Si_2Se_{1.22}S_{6.78}I$				
Element	Pr	Si	Se	S	I
Weight%	48.3	6.1	9.8	23.1	12.7
Atomic%	22.8	14.5	8.2	47.8	6.7
	$Nd_3Si_2Se_{1.18}S_{6.82}I$				
Element	Nd	Si	Se	S	I
Weight%	49.2	6.4	3.6	25.6	15.2
Atomic%	22.2	14.9	3.1	52.0	7.8

Table S2. Fractional atomic coordinates and atomic parameters.

$La_3Si_2Se_{1.21}S_{6.79}I$						
Atom	**Wyck.**	**Site**	**S.O.F.**	**x/a**	**y/b**	**z/c**
La1	8f	1		0.30268(2)	0.11939(2)	0.31844(2)
La2	4e	2		0	0.09470(2)	1/4
Si1	8f	1		0.16020(4)	0.03745(8)	0.02912(5)
S1	8f	1	0.649(2)	0.06602(2)	0.15741(5)	0.54243(3)
S2	8f	1	0.892(2)	0.14478(3)	0.24478(6)	0.14602(4)
S3	8f	1	0.897(2)	0.21811(3)	0.43077(6)	0.41523(4)
S4	8f	1	0.956(2)	0.34993(3)	0.39900(6)	0.15931(5)
Se1	8f	1	0.351(2)	0.06602(2)	0.15741(5)	0.54243(3)
Se2	8f	1	0.108(2)	0.14478(3)	0.24478(6)	0.14602(4)
Se3	8f	1	0.103(2)	0.21811(3)	0.43077(6)	0.41523(4)
Se4	8f	1	0.044(2)	0.34993(3)	0.39900(6)	0.15931(5)
I1	4e	2		0	0.51393(3)	1/4
$Ce_3Si_2Se_{1.39}S_{6.61}I$						
Atom	**Wyck.**	**Site**	**S.O.F.**	**x/a**	**y/b**	**z/c**
Ce1	8f	1		0.30182(2)	0.12028(2)	0.31787(2)
Ce2	4e	2		0	0.09532(2)	1/4
Si1	8f	1		0.16017(3)	0.03766(6)	0.02881(4)
S1	8f	1	0.6012(18)	0.06558(2)	0.15962(4)	0.54266(3)
S2	8f	1	0.8734(17)	0.14422(2)	0.24640(5)	0.14602(3)
S3	8f	1	0.8785(17)	0.21723(2)	0.43140(5)	0.41537(3)
S4	8f	1	0.9526(17)	0.35016(2)	0.39933(5)	0.16053(4)
Se1	8f	1	0.3988(18)	0.06558(2)	0.15962(4)	0.54266(3)
Se3	8f	1	0.1215(17)	0.21723(2)	0.43140(5)	0.41537(3)
Se2	8f	1	0.1266(17)	0.14422(2)	0.24640(5)	0.14602(3)
Se4	8f	1	0.0474(17)	0.35016(2)	0.39933(5)	0.16053(4)
I1	4e	2		0	0.51382(2)	1/4
$Pr_3Si_2Se_{1.22}S_{6.78}I$						
Atom	**Wyck.**	**Site**	**S.O.F.**	**x/a**	**y/b**	**z/c**
Pr1	8f	1		0.30176(2)	0.12067(2)	0.31796(2)
Pr2	4e	2		0	0.09729(2)	1/4
Si1	8f	1		0.16002(2)	0.03757(5)	0.02851(4)
S1	8f	1	0.6471(15)	0.06540(2)	0.16046(3)	0.54230(2)
S2	8f	1	0.8938(15)	0.14413(2)	0.24725(4)	0.14619(3)
S3	8f	1	0.8926(15)	0.21678(2)	0.43113(4)	0.41511(3)
S4	8f	1	0.9557(15)	0.35047(2)	0.39981(4)	0.16192(3)
Se1	8f	1	0.3529(15)	0.06540(2)	0.16046(3)	0.54230(2)
Se2	8f	1	0.1062(15)	0.14413(2)	0.24725(4)	0.14619(3)

Se3	8f	1	0.1074(15)	0.21678(2)	0.43113(4)	0.41511(3)
Se4	8f	1	0.0443(15)	0.35047(2)	0.39981(4)	0.16192(3)
I1	4e	2		0	0.51425(2)	1/4
$Nd_3Si_2Se_{1.18}S_{6.82}I$						
Atom	**Wyck.**	**Site**	**S.O.F.**	**x/a**	**y/b**	**z/c**
Nd2	4e	2		0	0.09814(2)	1/4
Nd1	8f	1		0.30123(2)	0.12100(2)	0.31799(2)
Si1	8f	1		0.15986(3)	0.03811(6)	0.02813(4)
S1	8f	1	0.6453(18)	0.06531(2)	0.16140(4)	0.54172(2)
S2	8f	1	0.9034(17)	0.14394(2)	0.24833(4)	0.14637(3)
S3	8f	1	0.9002(17)	0.21673(2)	0.43147(4)	0.41509(3)
S4	8f	1	0.9624(17)	0.35075(2)	0.39971(5)	0.16293(3)
Se1	8f	1	0.3547(18)	0.06531(2)	0.16140(4)	0.54172(2)
Se3	8f	1	0.0998(17)	0.21673(2)	0.43147(4)	0.41509(3)
Se2	8f	1	0.0966(17)	0.14394(2)	0.24833(4)	0.14637(3)
Se4	8f	1	0.0376(17)	0.35075(2)	0.39971(5)	0.16293(3)
I1	4e	2		0	0.51448(2)	1/4

Table S3. Interatomic distances of $Eu_2SiSe_xS_{4-x}$.

$La_3Si_2Se_{1.21}S_{6.79}I$			
La1	S3|Se3	1x	2.9529(5)
La1	S4|Se4	1x	2.9898(6)
La1	S3|Se3	1x	3.0161(5)
La1	S1|Se1	1x	3.0202(4)
La1	S4|Se4	1x	3.0635(6)
La1	S3|Se3	1x	3.0855(5)
La1	S2|Se2	1x	3.1082(5)
La1	S2|Se2	1x	3.1317(5)
La2	S4|Se4	1x	2.9420(5)
La2	S4|Se4	1x	2.9427(5)
La2	S2|Se2	1x	2.9877(5)
La2	S2|Se2	1x	2.9882(5)
La2	S1|Se1	1x	3.2842(3)
La2	S1|Se1	1x	3.2848(3)
La2	S1|Se1	2x	3.3183(4)
Si1	S4|Se4	1x	2.1157(8)
Si1	S2|Se2	1x	2.1244(8)
Si1	S3|Se3	1x	2.1547(8)
Si1	S1|Se1	1x	2.1908(7)
La•••La			4.5034(5)
I•••I			5.4966(4)
$Ce_3Si_2Se_{1.39}S_{6.61}I$			
Ce1	S3|Se3	1x	2.9338(4)
Ce1	S4|Se4	1x	2.9610(5)

Ce1	S3|Se3	1x	2.9999(4)
Ce1	S1|Se1	1x	3.0048(4)
Ce1	S4|Se4	1x	3.0360(5)
Ce1	S3|Se3	1x	3.0657(4)
Ce1	S2|Se2	1x	3.0869(4)
Ce1	S2|Se2	1x	3.1109(4)
Ce2	S4|Se4	1x	2.9201(4)
Ce2	S4|Se4	1x	2.9203(4)
Ce2	S2|Se2	2x	2.9641(4)
Ce2	S1|Se1	1x	3.2723(3)
Ce2	S1|Se1	1x	3.2726(3)
Ce2	S1|Se1	1x	3.3055(3)
Ce2	S1|Se1	1x	3.3057(3)
Si1	S4|Se4	1x	2.1132(6)
Si1	S2|Se2	1x	2.1234(6)
Si1	S3|Se3	1x	2.1547(6)
Si1	S1|Se1	1x	2.1956(6)
Ce1	S3|Se3	1x	2.9338(4)
Ce•••Ce			4.4610(5)
I•••I			5.4690(4)
$Pr_3Si_2Se_{1.22}S_{6.78}I$			
Pr1	S3|Se3	1x	2.9209(4)
Pr1	S4|Se4	1x	2.9403(4)
Pr1	S1|Se1	1x	2.9843(4)
Pr1	S3|Se3	1x	2.9865(4)
Pr1	S4|Se4	1x	3.0187(4)
Pr1	S3|Se3	1x	3.0470(4)
Pr1	S2|Se2	1x	3.0662(4)
Pr1	S2|Se2	1x	3.0932(4)
Pr2	S4|Se4	1x	2.9013(3)
Pr2	S4|Se4	1x	2.9020(3)
Pr2	S2|Se2	1x	2.9431(3)
Pr2	S2|Se2	1x	2.9437(3)
Pr2	S1|Se1	1x	3.2502(2)
Pr2	S1|Se1	1x	3.2505(2)
Pr2	S1|Se1	1x	3.3056(3)
Pr2	S1|Se1	1x	3.3058(3)
Si1	S4|Se4	1x	2.1143(5)
Si1	S2|Se2	1x	2.1215(5)
Si1	S3|Se3	1x	2.1512(5)
Si1	S1|Se1	1x	2.1874(5)
Pr•••Pr			4.4350(5)
I•••I			5.4450
$Nd_3Si_2Se_{1.18}S_{6.82}I$			
Nd2	S4|Se4	1x	2.8867(3)
Nd2	S4|Se4	1x	2.8874(3)
Nd2	S2|Se2	1x	2.9308(3)
Nd2	S2|Se2	1x	2.9314(3)
Nd2	S1|Se1	1x	3.2311(2)

Nd2	S1|Se1	1x	3.2314(2)
Nd2	S1|Se1	1x	3.3041(3)
Nd2	S1|Se1	1x	3.3043(3)
Nd1	S3|Se3	1x	2.9087(4)
Nd1	S4|Se4	1x	2.9225(4)
Nd1	S1|Se1	1x	2.9739(4)
Nd1	S3|Se3	1x	2.9744(4)
Nd1	S4|Se4	1x	3.0045(4)
Nd1	S3|Se3	1x	3.0294(4)
Nd1	S2|Se2	1x	3.0467(4)
Nd1	S2|Se2	1x	3.0776(4)
Si1	S4|Se4	1x	2.1115(5)
Si1	S2|Se2	1x	2.1187(6)
Si1	S3|Se3	1x	2.1467(6)
Si1	S1|Se1	1x	2.1857(6)
Nd•••Nd			4.4065(5)
I•••I			5.4067(4)

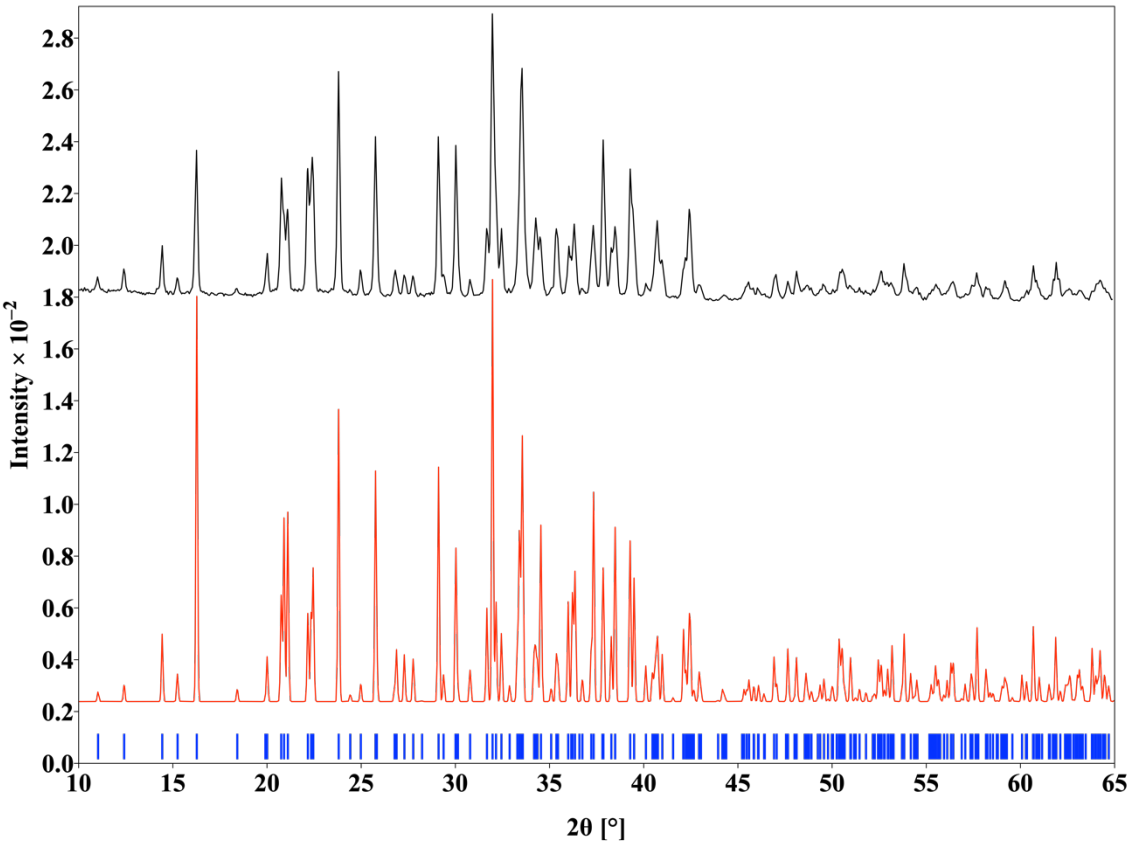

Figure S1. The PXRD pattern of polycrystalline $La_3Si_2Se_{1.21}S_{6.79}I$ compound (simulated pattern (black) experimental pattern (red) and Bragg position (blue)).

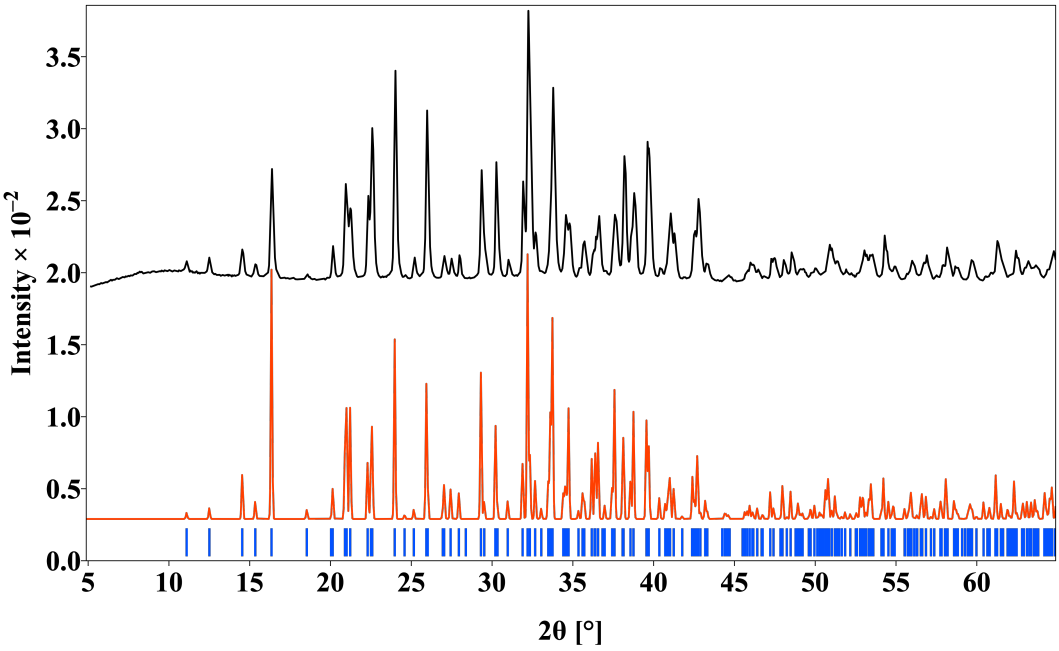

Figure S2. The PXRD pattern of polycrystalline $Ce_3Si_2Se_{1.39}S_{6.61}I$ compound (simulated pattern (black) experimental pattern (red) and Bragg position (blue)).

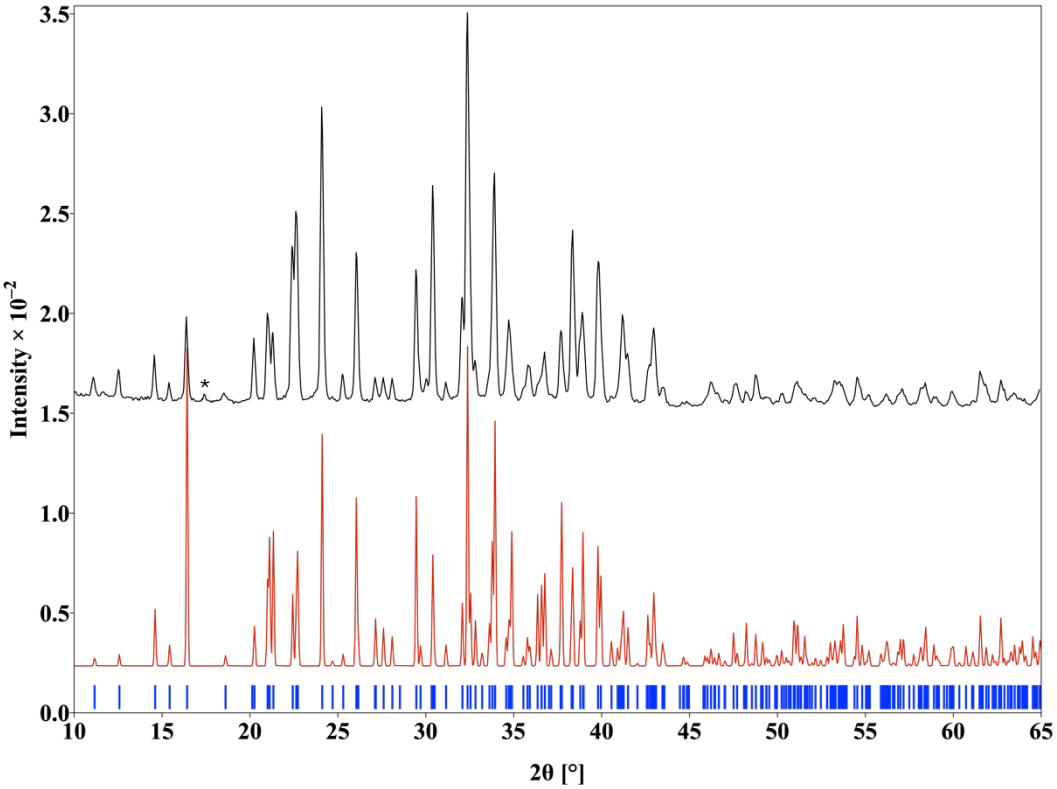

Figure S3. The pxrd pattern of polycrystalline $Pr_3Si_2Se_{1.22}S_{6.78}I$ compound (simulated pattern (black) experimental pattern (red) and Bragg position (blue)) (* unidentified peaks).

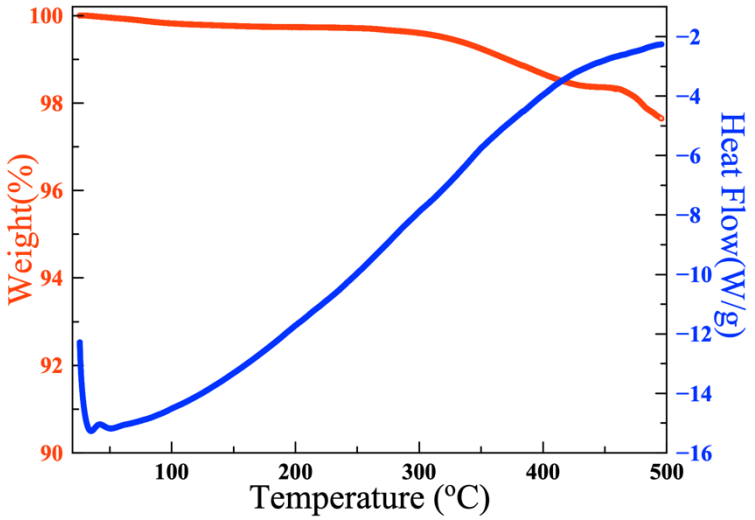

Figure. S4 TGA plot of polycrystalline $Ce_3Si_2Se_{1.39}S_{6.61}I$ under N_2 atmosphere.

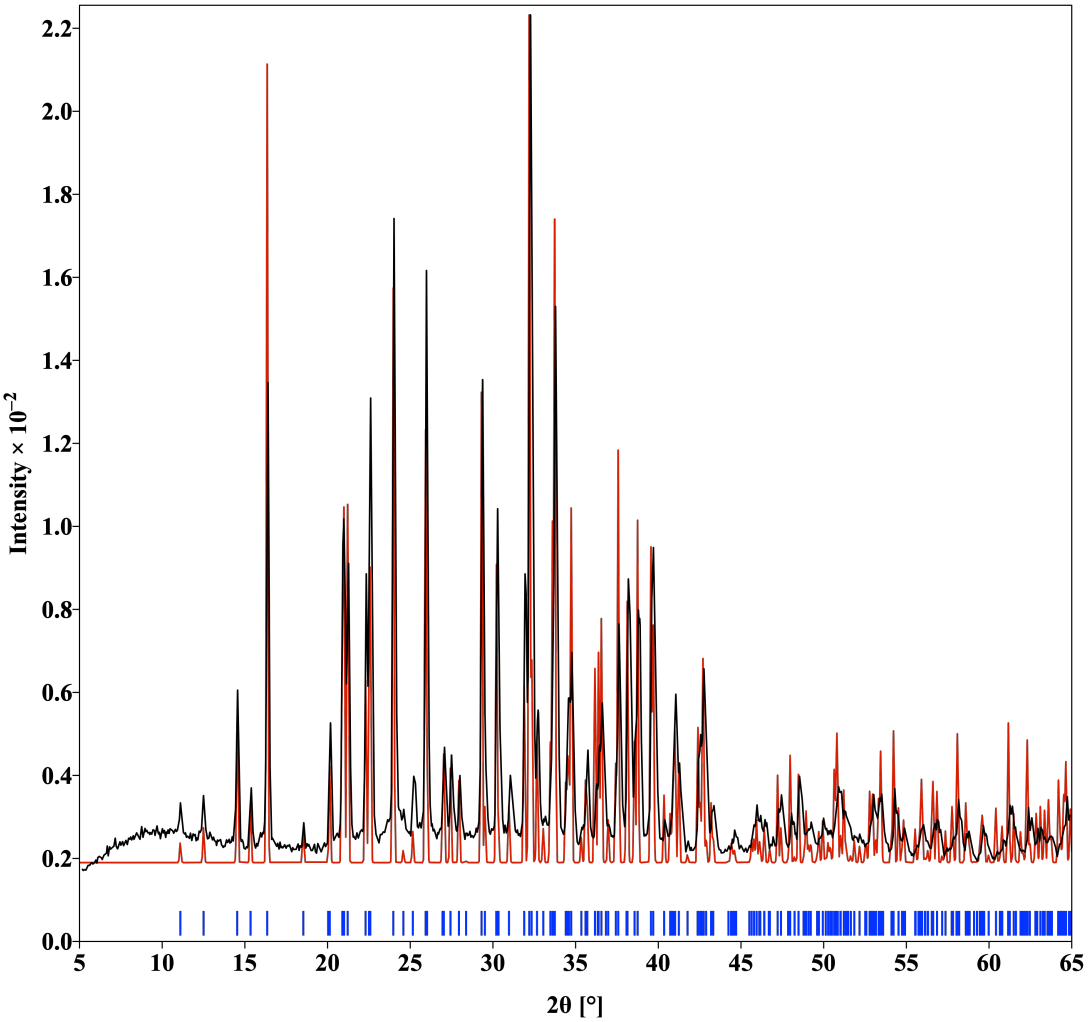

Figure S5. The PXRD pattern of polycrystalline $Ce_3Si_2Se_{1.39}S_{6.61}I$ compound after TGA experiment (experimental pattern (black) simulated pattern (red) and Bragg position (blue)).

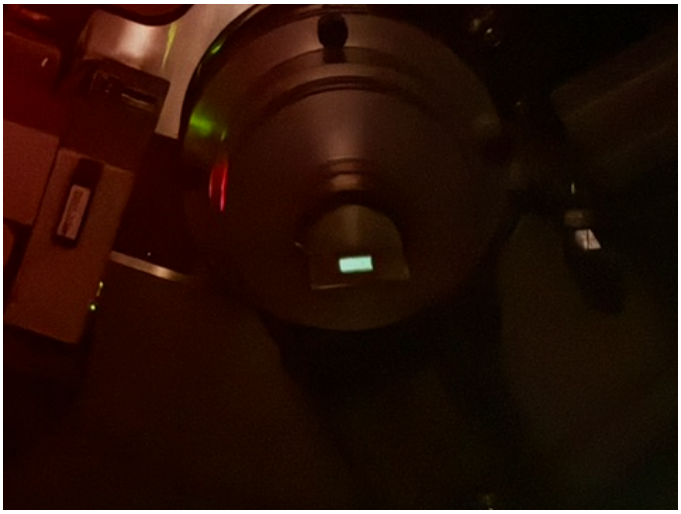

Figure S6. Scintillation of $Ce_3Si_2Se_{1.39}S_{6.61}I$ under exposer of X-ray

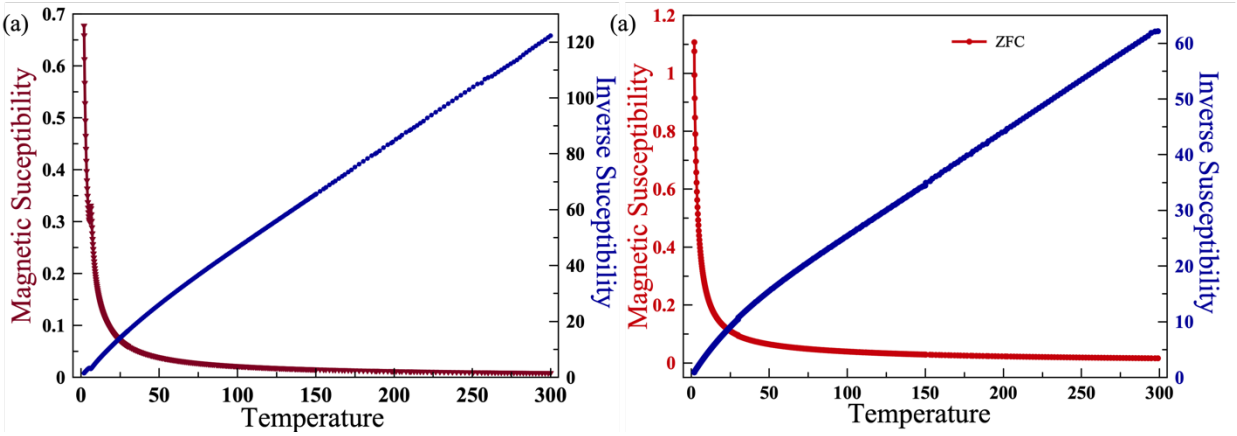

Figure S7. Molar and inverse molar magnetic susceptibility vs Temperature (ZFC) plots for (a) $Ce_3Si_2Se_{1.39}S_{6.61}I$ and (b) $Nd_3Si_2Se_{1.18}S_{6.82}I$.